Probing the pharmacokinetics of cucurbit[7, 8 and 10]uril: And a dinuclear ruthenium antimicrobial complex encapsulated in cucurbit[10]uril

Author

Li, Fangfei, Gorle, Anil K, Ranson, Marie, Vine, Kara L, Kinobe, Robert, Feterl, Marshall, Warner, Jeffrey M, Keene, F Richard, Collins, J Grant, Day, Anthony I

Published

2017

Journal Title

Organic and Biomolecular Chemistry

Version

Version of Record (VoR)

DOI

10.1039/c7ob00724h

Organic & Biomolecular Chemistry

PAPER

View Article Online
View Journal | View Issue

Cite this: Org. Biomol. Chem., 2017, 15, 4172

Probing the pharmacokinetics of cucurbit[7, 8 and 10]uril: and a dinuclear ruthenium antimicrobial complex encapsulated in cucurbit[10]uril†

Fangfei Li,[a] Anil K. Gorle,[a] Marie Ranson,[b] Kara L. Vine,[b] Robert Kinobe,[c,d] Marshall Feterl,[c,d] Jeffrey M. Warner,[c,d] F. Richard Keene, *[d,e] J. Grant Collins*[a] and Anthony I. Day *[a]

The relatively non-toxic family of cucurbit[*n*]uril, Q[*n*], have shown considerable potential *in vitro* as drug delivery agents, with only a few examples of pharmacokinetic (PK) studies for drug⊂Q[*n*]. Drug-free Q[*n*] PK studies are the next step in determining the pharmacological applicability in their drug delivery potential. The results for the first PK and bio-distribution of drug-free ^{14}C-Q[7] are described for administration *via* intravenous (i.v.) and intraperitoneal (i.p.) dosing. A study of oral administration of drug-free ^{14}C-Q[8] has also been undertaken to determine the time course for the gastrointestinal tract (GIT), absorption and subsequent bio-distribution. Q[10], a potential drug carrier for larger drugs, was evaluated for its effect on the PK profile of a dinuclear ruthenium complex ($Rubb_{12}$), a potential antimicrobial agent. The $Rubb_{12}$⊂Q[10] complex and free $Rubb_{12}$ were administered by i.v. to determine differences in $Rubb_{12}$ plasma concentrations and organ accumulation. Interestingly, the PK profiles and bio-distribution observed for Q[7] showed similarities to those of $Rubb_{12}$⊂Q[10]. Drug-free Q[7] has a relatively fast plasma clearance and a generally low organ accumulation except for the kidneys. Drug-free Q[8] showed a low absorption from the GIT into the blood stream but the small percentage absorbed reflected the organ accumulation of Q[7]. These results provide a better understanding of the probable PK profile and bio-distribution for a drug⊂Q[*n*] through the influence of the drug delivery vehicle and the positive clearance of drug-free Q[*n*] *via* the kidneys supports its potential value in future drug delivery applications.

Received 24th March 2017,
Accepted 20th April 2017

DOI: 10.1039/c7ob00724h

rsc.li/obc

Introduction

The family of macrocyclic host molecules known as cucurbit[*n*]uril (Q[*n*]); (see Fig. 1) has recently attracted considerable attention through the realisation of a wide-range of potential applications – including catalysis, the modification of electrochemical properties, the enhancement of some analytical processes, the synthesis of nano-materials and supramolecular polymers, for drug delivery and the modification of various biological processes.[1–16]

The Q[*n*] are available in a range of cavity sizes prescribed by the number of glycoluril moieties for a particular member (*n* = 5–8 and 10).[1–3] Other non-classical Q[*n*] members are also now available, including Q[13–15], which have limited cavities as a consequence of their twisted structures, in the form of Möbius strips.[17,18] The three Q[*n*] members that are of prime interest in the area of drug delivery are Q[7, 8 and 10], which have cavities large enough to accommodate drug molecules or parts of a drug molecule with cross-sections within the portal size ranges of 5.4–10.6 Å.[4–11,19] The hydrophobic regions of a drug are encapsulated within the hydrophobic cavity and electropositive groups can further stabilise encapsulation by electrostatic interactions with the carbonyl-rimmed portals. As encapsulation in Q[*n*] can increase the aqueous solubility of a drug, or reduce its toxicity or its degradation into non-active metabolites, Q[*n*] have been proposed as delivery vehicles for a

[a]School of Physical, Environmental and Mathematical Sciences, University of New South Wales, Australian Defence Force Academy, Canberra, ACT 2600, Australia. E-mail: g.collins@adfa.edu.au, a.day@adfa.edu.au
[b]School of Biological Sciences, Illawarra Health and Medical Research Institute, University of Wollongong, Wollongong, NSW 2522, Australia
[c]College of Public Health, Medical and Veterinary Sciences, James Cook University, Townsville, QLD 4811, Australia
[d]Centre for Biodiscovery and Molecular Development of Therapeutics, James Cook University, Townsville, QLD 4811, Australia
[e]School of Physical Sciences, University of Adelaide, Adelaide, SA 5000, Australia. E-mail: richard.keene@adelaide.edu.au

†Electronic supplementary information (ESI) available. See DOI: 10.1039/c7ob00724h

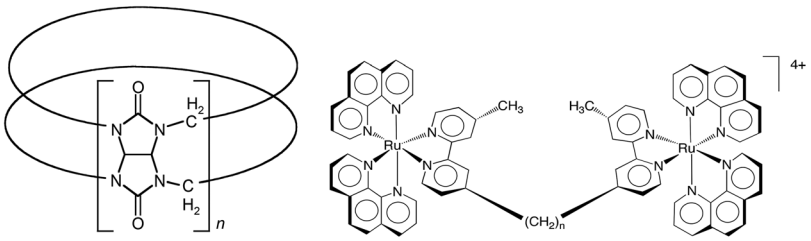

Fig. 1 The structure of cucurbit[*n*]uril (left-hand side) and Rubb$_n$ (right-hand side).

number of therapeutic drugs.[4–11,19–21] The drug delivery potential has been demonstrated experimentally *in vitro*, and in a few cases *in vivo*.[6,12,22,23] These are important as first steps in a pharmacological evaluation but the effect of the Q[*n*]-encapsulation on the pharmacokinetic (PK) profile (plasma concentration as a function of time and organ accumulation) of the drug *in vivo* is the next important determinant of the clinical potential of Q[*n*] as a drug delivery vehicle.[24–27] The Q[*n*] vehicle itself has already been shown to be relatively non-toxic.[28–31] To date there are few studies of the PK effect of encapsulated drugs in Q[*n*] and no studies on the PK of free Q[*n*]. The few examples of PK effects with drug⊂Q[*n*] include those by Ma *et al.* (oral administration)[32] and Plumb *et al.* (intraperitoneal administration)[33] of drugs encapsulated in Q[7] and have demonstrated improvements in plasma drug concentrations. A third example by Nguyen *et al.* (oral administration) of a drug/Q[6] nanoparticle also showed improved plasma drug concentrations.[34] However, it is not clear in these examples, whether it was the free drug after it was released from the host that diffuses into the blood stream in a sustained manner, or whether the drug encapsulated in Q[7] or Q[6] was carried into the plasma. It was anticipated that the study described herein, would help to answer this question through the PK profiling of free Q[7 and 8].

The increasing importance of Q[*n*] demonstrated by *in vivo* trials raises the significance of PK studies of free Q[*n*], especially for n = 7 and 8 as these cavity sizes have recently seen increasing potential as drug delivery hosts. In this context we present our results on the PK profiling of drug-free ^{14}C-labelled Q[7] and Q[8] with a focus on plasma clearance and organ accumulation. In addition, to determining the fate of Q[7 and 8] we also report a comparative PK profile of a relatively new potential antimicrobial agent encapsulated in Q[10], the largest available Q[*n*] cavity.[19] This antimicrobial agent is the inert dinuclear ruthenium(II) complex, $[\{Ru(phen)_2\}_2(\mu\text{-}bb_{12})]^{4+}$ {phen = 1,10-phenanthroline; bb_{12} = 1,12-bis[4(4′-methyl-2,2′-bipyridyl)]dodecane} ($Rubb_{12}$ – see Fig. 1, n = 12). The association complexes Rubb$_n$⊂Q[10] have $K_a > 10^9$ M^{-1},[32] and are therefore ideal candidates to evaluate the PK of Q[10] through the ready detection of ruthenium in plasma and organ samples by ICP-MS quantification.

The PK profiling of $Rubb_{12}$⊂Q[10] compared to free $Rubb_{12}$ provided data on the PK changes asserted upon the encapsulated drug and served to demonstrate parallels to the PK findings of a drug⊂Q[*n*] relative to free Q[7] and Q[8].

Results and discussion

Drug-free ^{14}C-labelled Q[7] and Q[8]

The few examples of published PK studies of Q[*n*] carrying a drug involved a determination of the fate of the drug but not the function (delivery potential and drug retention) or fate of the drug carrier. A delivered drug will inevitably leave an empty Q[*n*], which is a phenomenon that also needs to be understood in terms of PK.

Drug-free Q[7] has the highest intrinsic aqueous solubility of any of the classical Q[*n*] family (here "classical" refers to the original Q[*n*] without substituents) and drug-free Q[8] has an intrinsic solubility of <0.1 mM,[36] while the least soluble was drug-free Q[10] (~25 μM).[37] Drug-free Q[7] in clinical saline is soluble to ~35 mM, which makes this Q suitable for intravenous (i.v.) or intraperitoneal administration (i.p.) and PK profiling while carrying a ^{14}C-label. However, drug-free Q[8] with its lower solubility was considered only suitable for an oral PK study. The high stability of the Q[*n*], also supports its potential applicability to an oral route for drug delivery.[32,34] Q[8] and Q[10] are only very slightly increased in solubility in saline, although drug⊂Q[8 or 10] often have considerably higher aqueous solubility compared to the free host, with observed increases up to 100-fold for both.[35,38]

The radiolabelled ^{14}C-Q[7 and 8] were prepared by the acid-catalysed reaction of ^{14}C-paraformaldehyde with glycoluril under previously established unlabelled conditions.[39] Purification was achieved by a combination of dissolution and chromatography on cation exchange resin and each Q[*n*] verified by ^{1}H NMR.

The ^{14}C-Q[7] was assessed for its plasma clearance properties and organ uptake in Balb/c mice after i.p. administration, and in Sprague Dawley rats after i.v. administration. The i.p. plasma clearance in mice (Fig. 2a) appears to fit a 2-phase (2-compartment model) exponential decay curve, giving clearances of $t_{1/2}\alpha$ = 17.0 min and $t_{1/2}\beta$ = 270.7 min (half-lives for the two phases). Similarly i.v. administration in Sprague Dawley rats also fitted a multiphasic clearance model, where a $t_{1/2}\beta$ = 12.8 h, calculated from the linear 6–48 h post-dose interval (see ESI, plasma clearance Table S1, Fig. S1 and urine excretion Table S2†). It should be noted that the percentage of the injected i.p. dose was <30%, at maximum plasma concentration, and decreased relatively quickly.

In addition to plasma clearance, the bio-distribution of ^{14}C-Q[7] in mice following i.p. administration was also

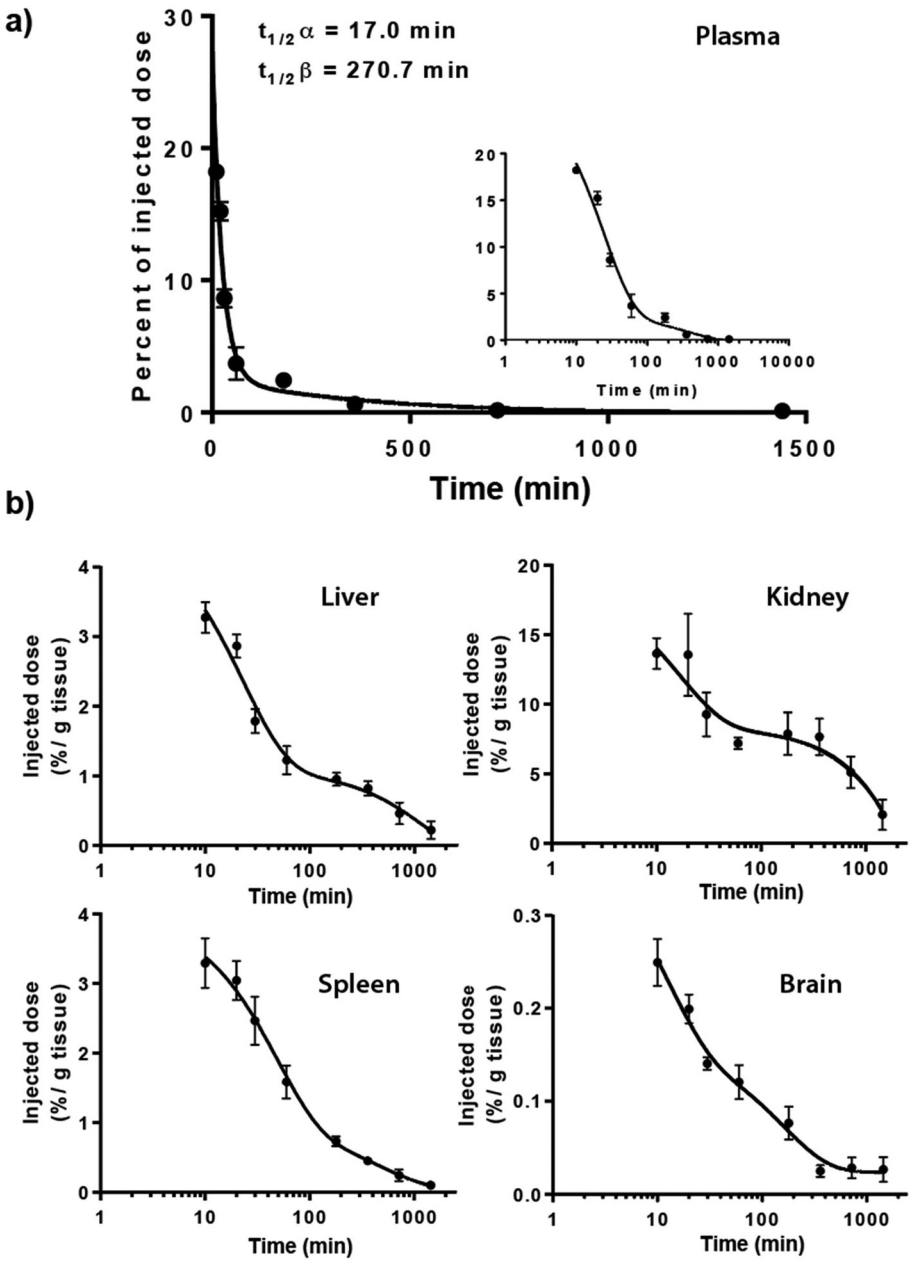

Fig. 2 Bio-distribution of ^{14}C-Q[7] in mice after i.p. administration. Percent of injected dose in plasma determined from t = 0–1440 min with the insert highlighting the period from 10 min, x-axis $\log_{10}$ and y-axis as percentage of injected dose corrected for the entire plasma volume (a); organ distribution (liver, kidneys, spleen and brain) t = 10–1440 min (b).

examined. Maximum organ accumulation of the ^{14}C-Q[7] was detected 10 min post-administration, in the spleen, liver and brain, while the kidneys saw two activity phases at ~20 and ~180 min (Fig. 2b). The large amount of activity detected in the kidneys (as opposed to the liver) suggests that Q[7] is renally excreted unchanged, possibly through glomerular filtration (in a fashion similar to β-cyclodextrin and hydroxypropyl-β-cyclodextrin).[40] Similarly, i.v. administration of ^{14}C-Q[7] in rats and urine sampling, at intervals within the periods 0–4, 4–8, 8–24 and 24–48 h, showed that approximately 50% of the excretion of ^{14}C-Q[7] occurred within the first 4 h. The total ^{14}C-Q[7] excreted over 48 h was 71.6% ± 16.5 of the total administered.

Low levels of ^{14}C-Q[7] were found accumulated in the spleen and liver (<4%, 10 min post-administration) in comparison to the plasma and kidneys (18.2% and 13.7% respectively, 10 min post-administration). The brain accumulated the least activity (<0.1% ± 0.06, over the entire duration of the study) suggesting that the ^{14}C-Q[7] does not cross the blood brain barrier.

Q[n] is potentially applicable for oral drug delivery in order to protect the drug from the harsh conditions of the

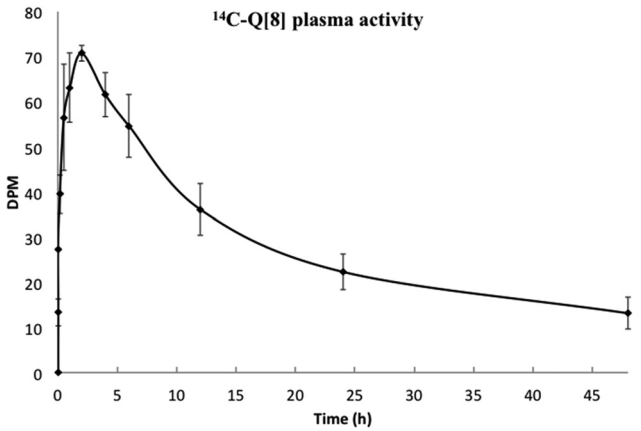

Fig. 3 Plasma concentrations of ^{14}C-Q[8] up to 48 h, following oral administration. Activity measured as disintegrations per minute (DPM) and maximum activity is ~0.001% of the dose.

gastrointestinal tract (GIT) and/or provide a mechanism for controlled adsorption into the blood stream. In this context we undertook a preliminary PK study of orally administered drug-free ^{14}C-Q[8]. A single bolus of a mix of labelled and unlabelled Q[8] was administered to Sprague Dawley rats and the bio-distribution established. Three time points of 2, 6 and 24 h were measured for the stomach, small and large intestines, liver, kidneys spleen, brain and bladder. Activity in the plasma was measured at 11 time points up to 48 h. The plasma activity *vs.* time profile showed limited absorption with a maximum concentration (~0.001% of the dose), obtained at ~2 h, followed by an elimination phase ($t_{1/2}\beta$ = 20 h) (Fig. 3). However, the total activity detected in the plasma was very low, consistent with the low urine recovery of 3.6% (of the total dose administered). Hence organ distribution was also low but proportionally similar to the results found in Fig. 2.

In contrast, a relatively high recovery of activity was measured from excreted faeces, 44.7% ± 20.4 of the total dose, with the largest proportion occurring in the 24–48 h period. The time course of activity for the passage through the GIT showed a peak at 2 h for stomach and the small intestine, followed by a peak at 6 h for the large intestine (see ESI Fig. S3†).

The low plasma activity and relatively high activity observed in the faeces and the GIT following oral dosing are consistent with a relatively poor absorption *via* this route. While drug free Q[8] may have low absorption from the GIT this does not exclude the value of the drug delivery vehicle from providing protection to the drug prior to release and absorption nor does it eliminate the possibility that a drug⊂Q[7 or 8] may have a different absorption profile, dependent upon the drug being carried.

PK profile of a Rubb$_{12}$⊂Q[10]

Rubb$_{12}$ (Fig. 1) as a potential antimicrobial agent is highly active against both Gram-positive and Gram-negative bacteria with retention of activity against drug-resistant strains, and it is non-toxic against healthy eukaryotic cells at concentrations well above its minimum inhibitory concentration (MIC).[41] As we have previously demonstrated Rubb$_{12}$ can form a high affinity, stable, water soluble complex with Q[10], and as such is suitable to evaluate the PK of Rubb$_{12}$⊂Q[10] and to compare this with the PK of the ruthenium complex.[19]

The maximum single dose tolerance (MTD) for free Rubb$_{12}$ and Rubb$_{12}$⊂Q[10] was established in mice following i.v. administration. It was found that encapsulation resulted in a two-fold decrease in toxicity for Rubb$_{12}$ (free – 1 mg kg^{-1}, encapsulated – 2 mg kg^{-1}). Using these dose limits, free Rubb$_{12}$ (1 mg kg^{-1}) was administered to mice by i.v. to establish the serum concentration profiles over a 12 h period post injection. A comparative group of mice were also administered with Rubb$_{12}$⊂Q[10] (equal quantity of Rubb$_{12}$) and serum concentrations of Rubb$_{12}$ were quantified using Inductively Coupled Plasma Mass Spectrum (ICP-MS) determination of the Ru concentrations. The results of the 12 h sampling of serum concentrations are shown in Fig. 4. After the initial equally rapid plasma clearance for both free and Q[10] bound Rubb$_{12}$, within the first 15 min of the exponential decay curve, there is a second clearance phase, which demonstrates a slightly slower clearance for Rubb$_{12}$⊂Q[10], $t_{1/2}\beta$ ~150 min (Fig. 4).

Of greater significance was the bio-distribution of the free Rubb$_{12}$ compared to Rubb$_{12}$⊂Q[10] in a range of organs, 6 h after the ruthenium complex had been administered by i.v. (Fig. 5). The primary site of accumulation for free Rubb$_{12}$ was the liver, with the kidneys, spleen, heart and lungs also exhibiting measurable quantities of ruthenium (~35% of injected dose). Interestingly, while free Rubb$_{12}$ accumulated predominantly in the liver, when administered as Rubb$_{12}$⊂Q[10] it was found to be distributed in comparable amounts in both the liver and kidneys. A substantial reduction (~2-times less) in accumulated complex in the liver was reflected by an increase in the kidneys (~4-fold). The other organs – spleen, heart lungs and brain – all showed lower levels of accumulated

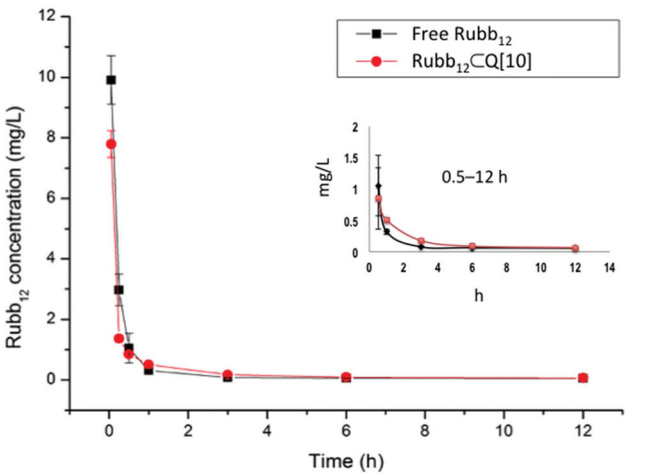

Fig. 4 The comparison of the serum level of free Rubb$_{12}$ and Rubb$_{12}$⊂Q[10] (1 mg kg^{-1} of drug) over 12 h after i.v. administration. The inset highlights the second phase of elimination over the period 0.5–12 h.

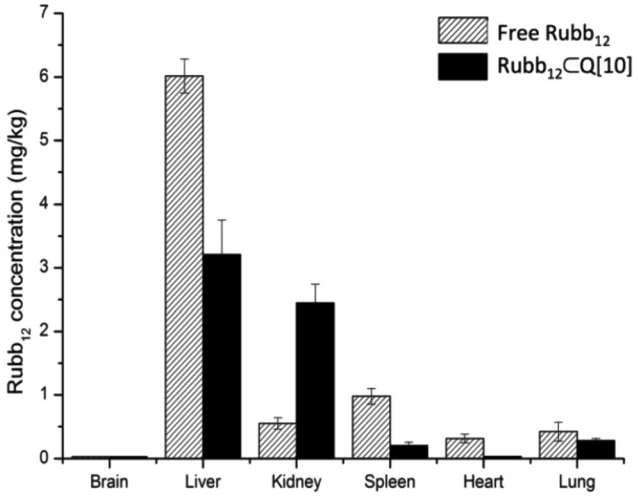

Fig. 5 Tissue accumulation of $Rubb_{12}$ after 6 h of a single dose at 1 mg kg^{-1} by i.v. injection of free $Rubb_{12}$ and $Rubb_{12}$⊂Q[10] in mice.

$Rubb_{12}$⊂Q[10] with the most notable differences found in the spleen and heart.

The very low accumulation in the heart as a result of encapsulation in Q[10] may have future significance in the case of drugs that have deleterious effects on heart tissue, as this finding may point to a method for limiting such negative effects of drugs delivered without encapsulation in Q[*n*].

Given the significant accumulation in the liver and the kidneys of $Rubb_{12}$, both free and encapsulated, a longer time course of up to 1 week was evaluated following a single i.v. injection. The results are shown in Fig. 6 reflecting a large percentage of the injected dose (~70%). The accumulation of ruthenium in the liver (Fig. 6a) reached a maximum level at 48 h for $Rubb_{12}$⊂Q[10] from which point the accumulated amount remained relatively constant up to 1 week. For free $Rubb_{12}$ it continues to accumulate from 6 h onwards, with levels doubling after 1 week.

Compared to the accumulation in the liver, the quantity of ruthenium found in the kidneys when delivered as the $Rubb_{12}$⊂Q[10] complex was maximal at 6 h and then steadily declined to half this level by 72 h up to 1 week, indicating a constant elimination (Fig. 6b). For the mice administered with free $Rubb_{12}$, accumulation of ruthenium in the kidneys slowly increased over time to a level similar to that of $Rubb_{12}$⊂Q[10] after 1 week following dosing.

These results demonstrate a higher accumulation and faster clearance of $Rubb_{12}$ through the kidneys when administered as the $Rubb_{12}$⊂Q[10] complex and a significant reduction in liver accumulation compared to administration of free $Rubb_{12}$. For an antimicrobial drug, a sufficient resident time within the body is desirable to complete its function but it is also important that it can be cleared from the body after serving its purpose. The positive clearance for $Rubb_{12}$⊂Q[10] from the body as shown in Fig. 6, demonstrates a desirable attribute imparted by Q[10] in its role as a potential drug delivery vehicle.

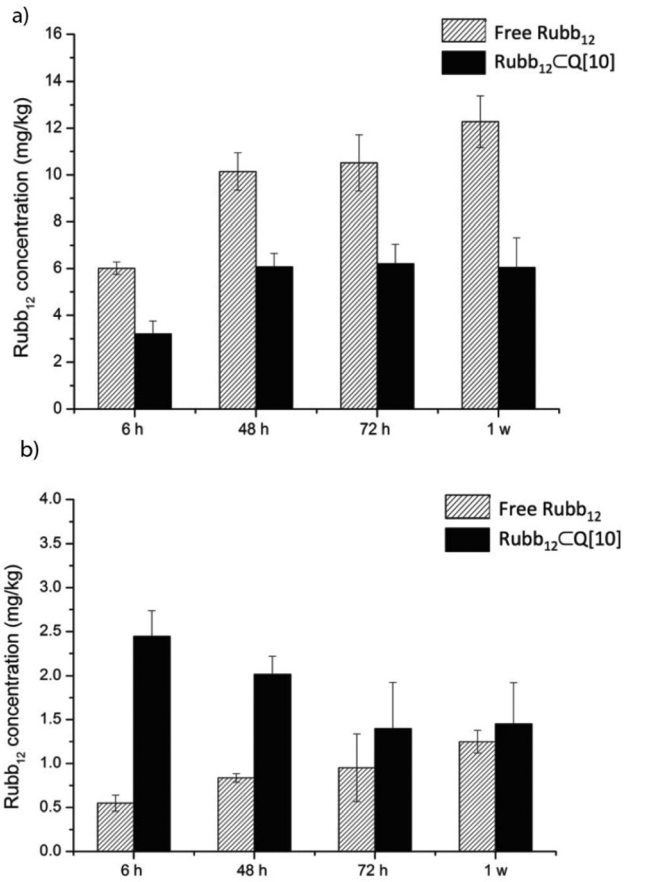

Fig. 6 The accumulation of $Rubb_{12}$ in the liver (a) and the kidneys (b) 6, 48, 72 h and 1 week after a single 1 mg kg^{-1} dose of free or $Rubb_{12}$⊂Q[10] by i.v. injection.

Conclusions

This study represents the first PK profile of the promising class of drug delivery vehicles Q[7 and 8] in the absence of a drug. In addition, we report the PK profiling of $Rubb_{12}$⊂Q[10] as a promising antimicrobial agent with improved PK when $Rubb_{12}$ is encapsulated in Q[10].

The acute toxicity study demonstrated that the MTD of $Rubb_{12}$ can be doubled when encapsulated as $Rubb_{12}$⊂Q[10], increasing the dose size from 1 to 2 mg kg^{-1}. This study provides the first data on the organ accumulation for a $Rubb_n$ complex.

The results with the ^{14}C-Q[7] provide strong evidence that the significant increase in kidney accumulation is due to the renal excretion of Q[*n*], rather than a specific effect of a drug⊂Q[*n*] complex. Consequently, it can be assumed that any drug administered as drug⊂Q[*n*] will show significant levels of accumulation in the kidneys driven largely by the Q[*n*] and less by the drug that it contains. However, the level of accumulation in other organs is likely to decrease also driven by the host Q[*n*]. The results of this study indicate that free Q[7] is relatively rapidly eliminated from the plasma when administered by either i.p. or i.v. routes, and from the study with

$Rubb_{12}$, encapsulated drugs will be eliminated from the plasma at a comparable rate to the free Q[*n*]. Encapsulation in Q[*n*] will affect the rate a drug enters the plasma after administration by non-intravenous routes. However, and importantly, encapsulation in Q[*n*] will modify the level of drug accumulation in various organs. This has potentially important implications for the toxicity of the encapsulated drug.

The results from oral administration of ^{14}C-Q[8] demonstrated that absorption of Q from the GIT into the blood stream is very low, and that the most likely application of drug⊂Q[*n*] is for protection and increased aqueous solubility to facilitate intestinal absorption. This suggestion is also supported by the reported improvements achieved for the drug triamterene⊂Q[7], which showed improved bioavailability and sustained plasma concentrations.[32]

Encapsulation in Q[10] with respect to plasma concentrations only led to a small increase in the concentration of $Rubb_{12}$, following the initial rapid concentration decrease to a linear elimination phase at ~30 min. After this point there was a slightly higher concentration of $Rubb_{12}$. Similarly, a reported, i.p. administered cisplatin⊂Q[7] complex decreased the maximum concentration in plasma, but slightly increased the concentration after the initial rapid build up of the drug following i.p. administration.[33]

The tissue distribution study demonstrated that the main site of accumulation for $Rubb_{12}$ is the liver, with considerable quantities also being found in the spleen and kidneys. The concentrations of $Rubb_{12}$ in the liver and kidneys were found to continually increase over time, up to one week after administration. This implies that the rapid clearance from the blood stream did not lead to a rapid excretion of $Rubb_{12}$ from the body, instead the complex concentrated in tissue as shown by the organ accumulation. Interestingly, $Rubb_{12}$⊂Q[10] exhibited a considerable lowering of accumulated $Rubb_{12}$ in most of the organs except for the kidneys. Significantly, the amount of $Rubb_{12}$ accumulating in the liver decreases, approximately 2-fold when administrated as $Rubb_{12}$⊂Q[10] and as the MTD was also improved, this may suggest that the main mechanism of toxicity of the $Rubb_{12}$ complexes was liver damage.

There are PK profile similarities between Q[7 and 8] and even without following the fate of free Q[10] directly, the $Rubb_{12}$⊂Q[10] complex exhibited a profile comparable to free Q[7 and 8]. Assuming that there was no significant chemical instability due to ^{14}C labelling,[42] these results suggest that the PK and bio-distribution will be dominated by the host for drugs⊂Q[7,8 and 10] where drug binding is relatively high.

Experimental

All the animal experiments were carried out in accordance with the institutional guidelines following approval from the respective animal ethics committees (University of Queensland Animal Ethics Committee Group 5) Project code TetraQ/059/09/NEWSOUTH; (James Cook University Animal Ethics Committee) App. no. A1753; (University of Wollongong Animal Ethics Committee) App. no. AE08/14.

Animals

Mixed-sex in-bred BALB/c mice aged 9–12 weeks were obtained from the small animal house located at the College of Public Health, Medical and Veterinary Sciences, James Cook University, Townsville, Australia.

Male Sprague Dawley rats 9–13 weeks were obtained from the Australian Institute of Bioengineering and Nanotechnology Animal House, University of Queensland.

In all studies food and water were available *ad libitum* throughout the life of the animals.

Synthesis of ^{14}C-labelled Q[7] and Q[8]

^{14}C-labelled Q[7] and Q[8] were prepared by our general cucurbit[*n*]uril synthetic method[39] on a scale where solid ^{14}C-paraformaldehyde (186.0 mg, 1 mCi, 37 MBq) was used in a reaction vial with HCl 32% (400 μL). After the reaction was complete the acid was completely removed and the dry solid residue treated with water (16 mL) at 90 °C cooled and centrifuged. The clear aqueous solution was separated from the solid plug. The water was evaporated at 60 °C and the residue purified on a short column of Dowex 50WX2 cation exchange resin, eluting with 0.5 M HCl/50% formic acid. The appropriate fractions yielded ^{14}C-cucurbit[7]uril 120 mg. The water insoluble material was suspended in 60% formic acid heated to 60 °C and then cooled. The remaining suspension was centrifuged. The solution was removed from the solid plug, which was then washed with a small volume of 60% formic acid and the centrifugation process repeated. The remaining solid was dried at 50 °C to give ^{14}C-cucurbit[8]uril (35 mg).

All samples of radiolabelled Q were stored as solids at −20 °C and used within a period of several months (the i.p. experiments were conducted with samples stored for <3 weeks) to minimise radiolytic decomposition.[42]

Intraperitoneal (i.p.) experiments with ^{14}C-Q[7]in mice

The intraperitoneal (i.p.) experiments with the free Q[7] were carried out using ^{14}C-Q[7] with BALB/c mice. Saturated solutions of ^{14}C-Q[7] were prepared in phosphate buffer saline (pH 7.4) by sonication, then heating to 95 °C cooled and filtered through 22 μm nylon syringe filters into sterile plastic sample tubes. Mice were injected (i.p.) with a single bolus dose (50 μL) of ^{14}C-Q[7] then sacrificed at 10, 20, 30, 60, 180, 360, 720 and 1440 min after injection. The total amount of activity injected per mouse was 4 μCi. Blood was immediately collected into tubes containing EDTA and plasma samples taken after centrifugation. Major organs were collected and weighed for further tissue/organ analysis. Samples were accurately weighed (between 0.1–0.5 g) and processed for liquid scintillation counting by incubation for 24 h at 60 °C with tissue solubiliser. Radioactivity was measured following mixing of the denatured homogenate sample with Packard Ultima Gold liquid scintillation counting cocktail (approximately 10 mL).

Intravenous (i.v.) experiments ^{14}C-Q[7] in rats

The i.v. administration experiments with ^{14}C-labelled Q[7] were carried out using Sprague Dawley rats. Blood samples were collected at 0, 2, 5, 10, 30 min, 1, 2, 4, 6, 12, 24 and 48 h post-dose into samples tubes containing the anti-coagulant lithium heparin. Samples were kept cold and centrifuged and the plasma transferred to a clean, polypropylene tubes. A 50–100 μL plasma aliquot was used to determine radioactivity.

Urine samples were collected at intervals pre-dose, 0–4 h, 4–8 h, 8–24 h and 24–48 h. Urine volume was determined by weighing. At the end of the 48 h period the collecting funnel was washed and the activity measured added to the total.

Oral experiments ^{14}C-Q[8] in rats

^{14}C-Q[8] was administered as a single bolus dose (2 mL kg^{-1}) as a water/PEG 400 solution (5 μCi of ^{14}C-Q[8] in 20 mg kg^{-1} cold Q[8]) by oral gavage. The animals were euthanased at three post-dose time points of 2, 6 24 h. The organs (stomach, small and large intestines, liver, kidneys, spleen whole brain and bladder) were excised, weighed and processed. Homogenated samples were accurately weighed (between 0.1–0.5 g) and processed for scintillation counting by incubation for 24 h at 60 °C with tissue solubiliser. Radioactivity was measured following mixing of the denatured homogenate sample with Packard Ultima Gold liquid scintillation-counting cocktail (approximately 10 mL).

Faeces collected during each time period were weighed and homogenised in 4 volumes of deionised water using a mechanical homogeniser. Approximately 0.1 to 1 g (accurately weighed) of this slurry was transferred to a 20 mL glass scintillation vial, 2 mL of tissue solubiliser added and the vials capped and incubated at 60 °C for at least 24 h.

The level of radioactivity in dose formulation, plasma (50 or 100 μL), urine (100 μL), faeces (0.1 to 1 g) and washout solution (100 μL) was added to scintillation vials containing Packard Ultima Gold liquid scintillation-counting cocktail (2.0 mL for plasma and dose, 5.0 mL for urine and cage washings, 10 mL for faeces).

Rubb$_{12}$ and Rubb$_{12}$⊂Q[10] *in vivo* experiments

Rubb$_{12}$ and Q[10] were prepared as previously described.[19]

Pharmokinetic analysis of Rubb$_{12}$

Preliminary acute toxicity (tolerability) studies. To enable appropriate doses of Rubb$_{12}$ to be used in the pharmacokinetic studies, the maximum tolerated single dose was determined in the BALB/c mouse strain. Groups of three mice, containing at least one male and one female, received intravenous (i.v.) doses of Rubb$_{12}$ or Rubb$_{12}$⊂Q[10]. The doses ranged from 0.4 to 4 mg kg^{-1} by the i.v. route and animals were closely monitored for 24 h. Mice exhibiting clinical adverse event signs were euthanased *via* CO_2 asphyxiation. The maximum tolerated single dose was recorded as the highest dose that was given to a group of mice where there was no mortality and no clinical adverse event signs.

Dosing and sampling. In all the studies, three mice were sampled at each of the time points. An untreated control group of three mice were sacrificed and the blood sampled as the 0 h time point. Rubb$_{12}$ and Rubb$_{12}$⊂Q[10] were dissolved in sterile PBS solution at the appropriate concentrations to obtain the desired doses relative to the Rubb$_{12}$. Rubb$_{12}$ solutions, (approximately 200 μL) were administered to the mice at 1 mg kg^{-1} intravenously (i.v.), as boluses to the mice through a 26.5-gauge needle, into a tail vein. After administration, blood was sampled at 0, 0.25, 0.5, 1, 3, 6, 12 h after dosing, and the brain, heart, lungs, liver, kidney (left side) and spleen were collected from mice 6, 48, 72 h and 1 week after a single dose.

Blood was collected from the mice by cardiac puncture immediately after they were sacrificed and then transferred to 1.7 mL eppendorf micro-centrifuge tubes. The samples were kept in the fridge at 4 °C until the blood was completely clotted and then the serum was separated by centrifugation at 3000*g* for 5 min. Tissues were washed with sterile PBS and weighed. Serum and tissue samples were stored at −20 °C until analysis.

Sample preparation and digestion. Blood serum samples were thawed and diluted 20-fold in Milli-Q water for ICP-MS analysis. Organ samples were digested using a microwave oven (Milestone Starter D). Fresh samples were placed in a digestion vessel, SupraPure double-distilled 65% HNO_3 (3 mL), AR Grade H_2O_2 (1 mL) and Milli-Q water (4 mL) added and the mixture was left in the fume hood for 2 h to digest the organ. The vessel was then loaded into the microwave oven, and heated to 180 °C for 10 min. After cooling, the digested samples were quantitatively transferred into a 100 mL volumetric flask and diluted to the mark using Milli-Q water. These solutions were diluted 2-fold before ICP-MS analysis.

Ruthenium concentration determination by ICP-MS. Sample analysis was carried out using a Bruker 820-MS Inductively Coupled Plasma Mass Spectrometer. A ruthenium standard (1000 mg L^{-1} ruthenium in 2% HCl) was used for calibration. The concentrations of ^{99}Ru and ^{101}Ru were measured and the ^{101}Ru isotope was used for quantification. A 20 ppb solution of the ruthenium standard was used to calibrate the instrument, indium was used as an internal standard to correct for the instrument drift and matrix effects. A 5 ppb independent ruthenium standard was used as the quality control sample.

Acknowledgements

We thank TetraQ, University of Queensland, for the ^{14}C-Q[7 and 8] i.v. and oral animal data collection, NewSouth Innovations for funding support through a COMET Grant 2009 and a NHMRC Development Grant application 514644 to M. Ranson.

References

1 K. I. Assaf and W. M. Nau, *Chem. Soc. Rev.*, 2015, **44**, 394–418.
2 L. Isaacs, *Acc. Chem. Res.*, 2014, **47**, 2052–2062.

3 E. Masson, X. Ling, R. Joseph, L. Kyeremeh-Mensah and X. Lu, *RSC Adv.*, 2012, **2**, 1213–1247.
4 J. Liu, Y. Lan, Z. Yu, C. S. Y. Tan, R. M. Parker, C. Abell and O. A. Scherman, *Acc. Chem. Res.*, 2017, **50**, 208–217.
5 J. Liu, C. S. Y. Tan, Y. Lan and O. A. Scherman, *Macromol. Chem. Phys.*, 2016, **217**, 319–332.
6 X. Ma and Y. Zhao, *Chem. Rev.*, 2015, **115**, 7794–7839.
7 N. Saleh, I. Ghosh and W. M. Nau, in *Supramolecular Systems in Biomedical Fields*, ed. H.-J. Schneider, Royal Society of Chemistry, 2013, ch. 7, pp. 164–212.
8 V. Saluja and B. S. Sekhon, *J. Pharm. Educ. Res.*, 2013, **4**, 16–25.
9 I. Ghosh and W. M. Nau, *Adv. Drug Delivery Rev.*, 2012, **64**, 764–783.
10 A. I. Day and J. G. Collins, in *Supramolecular Chemistry from molecules to nanomaterials*, ed. J. W. Steed and P. A. Gale, John Wiley & Sons Ltd, Chichester, UK, 2012, vol. 3, pp. 983–1000.
11 S. Walker, R. Oun, F. J. McInnes and N. J. Wheate, *Isr. J. Chem.*, 2011, **51**, 616–624.
12 D. H. Macartney, *Future Med. Chem.*, 2013, **5**, 2075–2089.
13 A. A. Elbashir and H. Y. Aboul-Enein, *Crit. Rev. Anal. Chem.*, 2015, **45**, 52–61.
14 A. E. Kaifer, *Acc. Chem. Res.*, 2014, **47**, 2160–2167.
15 J. P. Da Silva, R. Choudhury, M. Porel, U. Pischel, S. Jockusch, P. C. Hubbard, V. Ramamurthy and A. V. Canario, *ACS Chem. Biol.*, 2014, **9**, 1432–1436.
16 H. H. Lee, T. S. Choi, S. J. Lee, J. W. Lee, J. Park, Y. H. Ko, W. J. Kim, K. Kim and H. I. Kim, *Angew. Chem., Int. Ed.*, 2014, **53**, 7461–7465.
17 Q. Li, S.-C. Qiu, J. Zhang, K. Chen, Y. Huang, X. Xiao, Y. Zhang, F. Li, Y.-Q. Zhang, S.-F. Xue, Q.-J. Zhu, Z. Tao, L. F. Lindoy and G. Wei, *Org. Lett.*, 2016, **18**, 4020–4023.
18 X.-J. Cheng, L.-L. Liang, K. Chen, N.-N. Ji, X. Xiao, J.-X. Zhang, Y.-Q. Zhang, S.-F. Xue, Q.-J. Zhu, X.-L. Ni and Z. Tao, *Angew. Chem., Int. Ed.*, 2013, **52**, 7252–7255.
19 F. Li, M. Feterl, J. M. Warner, A. I. Day, F. R. Keene and J. G. Collins, *Dalton Trans.*, 2013, **42**, 8868–8877.
20 H. Chen, J. Y. W. Chan, S. Li, J. J. Liu, I. W. Wyman, S. M. Y. Lee, D. H. Macartney and R. Wang, *RSC Adv.*, 2015, **5**, 63745–63752.
21 Y. Xue, Z. Wang, Y. Niu, X. Chen, S. M. Y. Lee and R. Wang, *Chem. Med. Comm.*, 2016, **7**, 1392–1397.
22 Y. Chen, Z. Huang, H. Zhao, J.-F. Xu, Z. Sun and X. Zhang, *ACS Appl. Mater. Interfaces*, 2017, **9**, 8602–8608.
23 S. Li, J. Y.-W. Chan, Y. Li, D. Bardelang, J. Zheng, W. W. Yew, D. P.-C. Chan, S. M. Y. Lee and R. Wang, *Org. Biomol. Chem.*, 2016, **14**, 7563–7569.
24 M. J. Webber, E. A. Appel, B. Vinciguerra, A. B. Cortinas, L. S. Thapa, S. Jhunjhunwala, L. Isaacs, R. Langer and D. G. Anderson, *Proc. Natl. Acad. Sci. U. S. A.*, 2016, **113**, 14189–14194.
25 X. Miao, Y. Li, I. Wyman, S. M. Y. Lee, D. H. Macartney, Y. Zheng and R. Wang, *MedChemComm*, 2015, **6**, 1370–1374.
26 Q.-L. Li, Y. Sun, Y.-L. Sun, J. Wen, Y. Zhou, Q.-M. Bing, L. D. Isaacs, Y. Jin, H. Gao and Y.-W. Yang, *Chem. Mater.*, 2014, **26**, 6418–6431.
27 R. Oun, J. A. Plumb and N. J. Wheate, *J. Inorg. Biochem.*, 2014, 1100–134105.
28 R. Oun, R. S. Floriano, L. Isaacs, E. G. Rowan and N. J. Wheate, *Toxicol. Res.*, 2014, **3**, 447–455.
29 G. Hettiarachchi, D. Nguyen, J. Wu, D. Lucas, D. Ma, L. Isaacs and V. Briken, *PLoS One*, 2010, **5**, e10514.
30 V. D. Uzunova, C. Cullinane, K. Brix, W. M. Nau and A. I. Day, *Org. Biomol. Chem.*, 2010, **8**, 2037–2042.
31 H. Chen, J. Y. W. Chan, X. Yang, I. W. Wyman, D. Bardelang, D. H. Macartney, S. M. Y. Lee and R. Wang, *RSC Adv.*, 2015, **5**, 30067–30074.
32 W.-J. Ma, J.-M. Chen, L. Jiang, J. Yao and T.-B. Lu, *Mol. Pharmaceutics*, 2013, **10**, 4698–4705.
33 J. A. Plumb, B. Venugopal, R. Oun, N. Gomez-Roman, Y. Kawazoe, N. S. Venkataramanan and N. J. Wheate, *Metallomics*, 2012, **4**, 561–567.
34 T. H. Nguyen, P. T. T. Dao, Q. N. Phu, D. D. Le, T. A. Nguyen, T. C. Nguyen and M. C. Dang, *Adv. Nat. Sci.: Nanosci. Nanotechnol.*, 2012, **3**, 045004.
35 M. J. Pisani, Y. Zhao, L. Wallace, C. E. Woodward, F. R. Keene, A. I. Day and J. G. Collins, *Dalton Trans.*, 2010, **39**, 2078–2086.
36 L. M. Heitmann, A. B. Taylor, P. J. Hart and A. R. Urbach, *J. Am. Chem. Soc.*, 2006, **128**, 12574–12581.
37 This solubility was determined for acid free Q[10] in pure water.
38 Y. Zhao, M. H. Pourgholami, D. L. Morris, J. G. Collins and A. I. Day, *Org. Biomol. Chem.*, 2010, **8**, 3328–3337.
39 A. I. Day, A. P. Arnold, R. J. Blanch and B. Snushall, *J. Org. Chem.*, 2001, **66**, 8094–8100.
40 Y. Kubota, M. Fukuda, M. Muroguchi and K. Koizumi, *Biol. Pharm. Bull.*, 1996, **19**, 1068–1072.
41 A. K. Gorle, X. Li, S. Primrose, F. Li, M. Feterl, R. T. Kinobe, K. Heimann, J. M. Warner, F. R. Keene and J. G. Collins, *J. Antimicrob. Chemother.*, 2016, **71**, 1547–1555.
42 A. Fredenhagen, *J. Labelled Compd. Radiopharm.*, 2003, **46**, 211–220.